NMR Spectroscopy

International Edition: DOI: 10.1002/anie.201606594
German Edition: DOI: 10.1002/ange.201606594

^{1}H-Detected Solid-State NMR Studies of Water-Inaccessible Proteins In Vitro and In Situ

*João Medeiros-Silva, Deni Mance, Mark Daniëls, Shehrazade Jekhmane, Klaartje Houben, Marc Baldus, and Markus Weingarth**

Abstract: *^{1}H detection can significantly improve solid-state NMR spectral sensitivity and thereby allows studying more complex proteins. However, the common prerequisite for ^{1}H detection is the introduction of exchangeable protons in otherwise deuterated proteins, which has thus far significantly hampered studies of partly water-inaccessible proteins, such as membrane proteins. Herein, we present an approach that enables high-resolution ^{1}H-detected solid-state NMR (ssNMR) studies of water-inaccessible proteins, and that even works in highly complex environments such as cellular surfaces. In particular, the method was applied to study the K^+ channel KcsA in liposomes and in situ in native bacterial cell membranes. We used our data for a dynamic analysis, and we show that the selectivity filter, which is responsible for ion conduction and highly conserved in K^+ channels, undergoes pronounced molecular motion. We expect this approach to open new avenues for biomolecular ssNMR.*

Proton (^{1}H) detection can greatly increase spectral sensitivity in solid-state NMR (ssNMR) spectroscopy and thereby enables the study of complex proteins.[1] ^{1}H-detected ssNMR experiments usually require a stark dilution of the ^{1}H network to diminish line-broadening dipolar ^{1}H–^{1}H couplings, which can be achieved by protein expression in deuterated solvents.[2] Whereas such high degrees of deuteration can provide excellent ^{1}H resolution, they necessitate a proton/deuterium (H/D) back-exchange step to incorporate amino protons (H^N). Consequently, with these labeling techniques, water-inaccessible protein regions remain invisible for ^{1}H detection unless unfolding and refolding protocols are used, which are tedious, not broadly applicable, and limited to in vitro preparations. Moreover, deuterated solvents can reduce or prevent protein expression, especially in mammalian cells, and are generally associated with high costs for low-yield proteins. A remedy to these problems would be the use of fully protonated proteins;[3] however, such systems often provide limited spectral resolution. Even at very fast magic angle spinning (MAS) frequencies (> 100 kHz),[4] the resolution in fully protonated samples is governed by residual ^{1}H–^{1}H couplings. Moreover, the sensitivity loss that is due to the small sample volumes required for > 100 kHz MAS may not be compensated for in heterogeneous systems such as cellular samples.

These issues have thus far critically limited the application of ^{1}H detection for the study of water-inaccessible protein regions, which is a major obstacle for ssNMR spectroscopy as binding pockets and active sites alike can be buried deep inside protein cores, far away from the bulk water. It is a particularly severe problem for the study of membrane proteins, whose transmembrane (TM) parts are critical for their function and do not undergo exchange in protonated buffers.[2c,3c,5] This prompted us to develop a two-step approach that is generally applicable in vitro and in situ, works already at moderate MAS frequencies of 60 kHz, and provides well-resolved ^{1}H-detected NMR spectra of water-inaccessible protein regions. In the first step, we enhance the ^{1}H resolution by employing a novel labeling scheme, dubbed inverse fractional deuteration (iFD), which is based on protonated solvents (100 % H_2O) and fully deuterated [^{13}C]glucose in the growth medium. In the second step, we wash the iFD-labeled protein with deuterated buffers (100 % D_2O), which further markedly improves the spectral resolution. We first studied the iFD labeling approach on ubiquitin and then, in combination with the D_2O wash, used it to assign the TM part of the ion channel KcsA in lipid bilayers. Based on our assignments, we present a site-resolved study of the dynamics of the TM part, which is crucial to fully understand ion channel gating. Remarkably, our approach even provides sufficient spectral quality for the site-resolved analysis of a membrane protein in situ, that is, directly in a native bacterial cell membrane.

iFD labeling is the first of two consecutive steps to improve the resolution of water-inaccessible protons, especially for H^N and Hα, which are most important for backbone assignments. ^{1}H-detected 2D NH and CH spectra of iFD-labeled [^{13}C,^{15}N]ubiquitin in aqueous (100 % H_2O) buffers, acquired at 60 kHz MAS and 950 MHz ^{1}H frequency using MISSISSIPI water suppression[7] and PISSARRO decoupling,[8] are shown in Figures 1 A, B. These spectra are very well resolved and feature an average linewidth of 0.1–0.2 ppm for H^N and Hα at 950 MHz, which is excellent considering the high ^{1}H density of 80 % in iFD proteins, and constitutes a substantial average linewidth improvement of about 30–35 % compared to fully protonated ubiquitin (see Figure 1 C

[*] J. Medeiros-Silva, D. Mance, M. Daniëls, S. Jekhmane, Dr. K. Houben, Prof. M. Baldus, Dr. M. Weingarth
NMR Spectroscopy, Bijvoet Center for Biomolecular Research
Department of Chemistry, Utrecht University
Pandualaan 8, 3584 CH Utrecht (The Netherlands)
E-mail: M.H.Weingarth@uu.nl

Supporting information for this article can be found under: http://dx.doi.org/10.1002/anie.201606594.

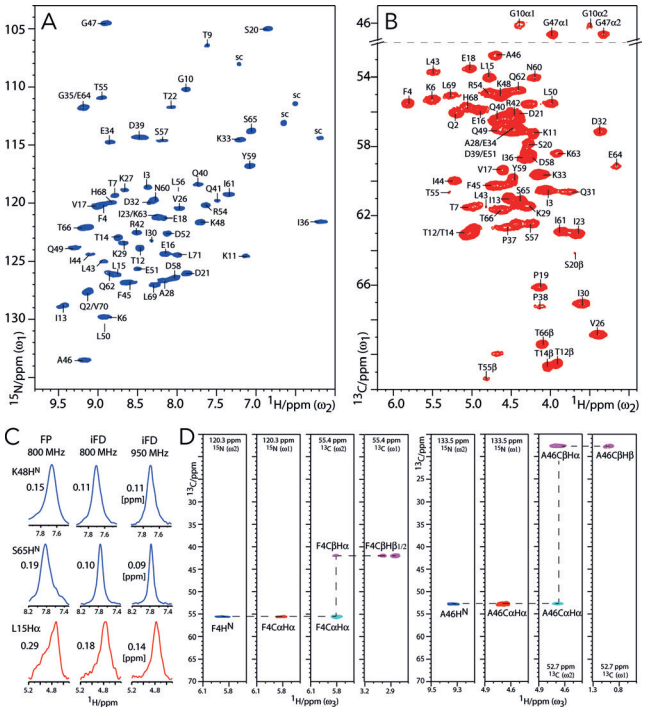

Figure 1. Dipolar ^{1}H-detected ssNMR experiments in iFD ubiquitin measured at 950 MHz and 60 kHz MAS. A) 2D NH spectrum (blue). B) CαHα region of a 2D CH spectrum (red). C) t_1 cross-sections extracted from 2D NH (blue) and CH (red) spectra of fully protonated (FP) and iFD ubiquitin. D) ^{1}H-detected side-chain assignments. Strip plots are shown for 3D CαNH (blue), 3D NCαHα (red), and 3D CCH (cyan and magenta for negative and positive signals, respectively) experiments. DREAM[6] ^{13}C–^{13}C transfer was used for the 3D CCH experiment.

and the Supporting Information, Table S1; see also Section S2 for a quantitative ^{1}H population analysis and a discussion of the ^{1}H linewidth improvement). Moreover, as both Hα and, obviously, H^N are recruited from the protonated solvent during protein expression, their ^{1}H levels are close to 100 % in iFD ubiquitin. We also observed a very good resolution of around 0.1 ppm for many side-chain ^{1}H (Figure S3), although the resolution of certain methyl groups was compromised by isotopologue effects. Hence, owing to the high ^{1}H density and ^{1}H resolution in iFD ubiquitin, the backbone and many side-chain protons could be readily assigned (Figure 1 D). We first correlated backbone H^N that had been previously assigned[2f] and Hα protons using 3D CαNH and NCαHα experiments. We then used a 3D CCH experiment to detect side-chain ^{1}H, which were connected to backbone H^N via the Hα protons (see the Supporting Information for experimental details).

To further improve the ^{1}H resolution of water-inaccessible protein regions, we combined iFD labeling with a D_2O wash. This was demonstrated with the K^+ channel KcsA, a well-accepted model for ion channel gating.[9] Figure 2 A shows a 2D NH spectrum of iFD/[^{13}C,^{15}N]-labeled KcsA, reconstituted in *E. coli* lipids and protonated buffers, acquired at 60 kHz MAS and 800 MHz. This spectrum, which shows the H^N signals of the entire channel, is already of superior resolution compared to our earlier results with fully proton-

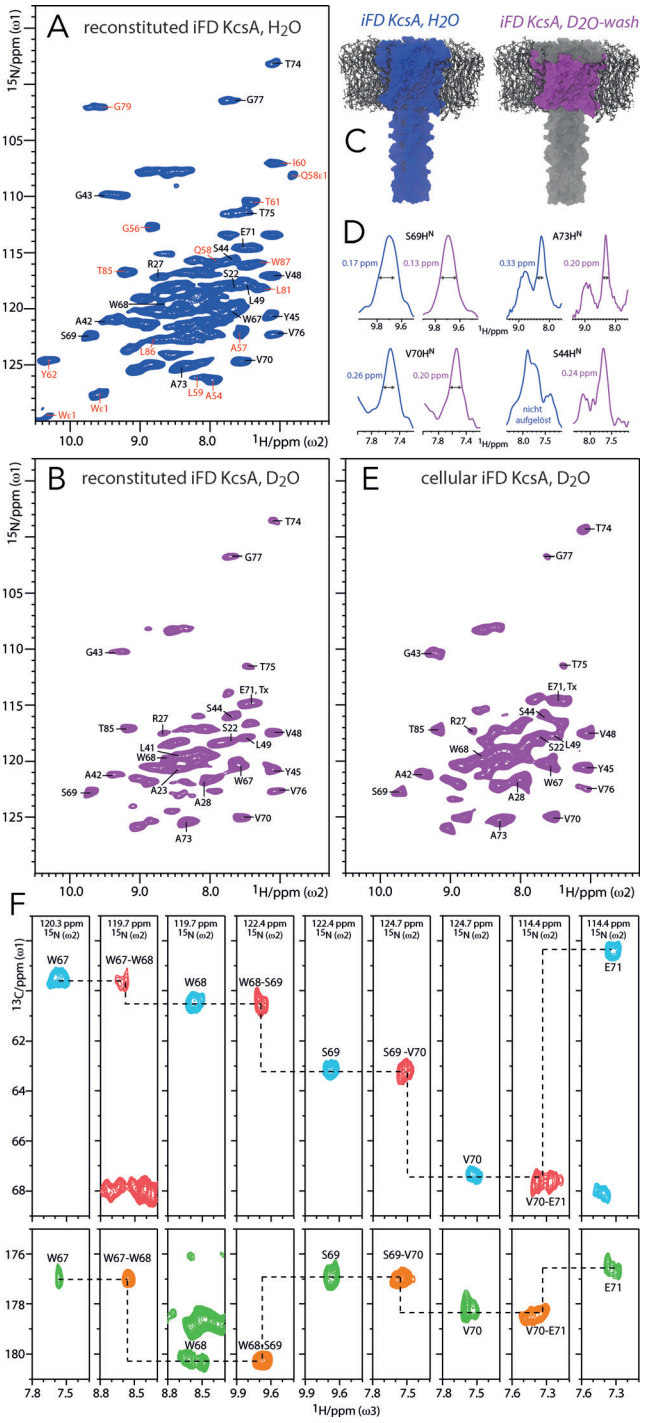

Figure 2. ^{1}H detection of water-inaccessible regions in the ion channel KcsA. All data were recorded at 60 kHz MAS and 800 MHz. 2D NH spectra of reconstituted iFD KcsA A) before (blue) and B) after a D_2O wash (magenta), and of E) cellular D_2O-incubated iFD KcsA, measured in native cell membranes (magenta). Assignments in red and black were obtained with FD KcsA[2f] and iFD KcsA, respectively. C) Color coding of regions that feature detectable H^N. All H^N are present in iFD KcsA whereas only the TM ones remain after the D_2O wash. D) t_1 cross-sections extracted from 2D NH spectra of iFD KcsA before (blue) and after (magenta) a D_2O wash. F) ^{1}H-detected assignments of residues W67–E71 of the pore helix. Strip plots are shown for 3D CαNH (cyan), Cα(CO)NH (red), CONH (orange), and CO(Cα)NH (green) experiments.

ated KcsA,[3c] and readily allows identifying previously assigned water-exposed signals (red, Figure 2A).[2f] To exclusively select the TM part, we incubated iFD-labeled KcsA in D_2O and acquired a 2D NH spectrum, which featured a stark enhancement in spectral quality with well-resolved signals as narrow as 0.13 ppm (Figures 2B,C). The resolution improvement is partly due to the virtually complete disappearance of the water-exposed residues, which reduces spectral congestion (see Figure S4 for a spectral overlay). Remarkably, the removal of water protons (and other exchangeable ^1H) further narrows the linewidth of the TM H^N by 25% on average compared to the spectrum shown in Figure 2A (Figure 2D and Table S5). The latter has not been observed before in ssNMR spectroscopy, and implies that residual dipolar couplings to water protons can contribute to the ^1H linewidth in highly protonated membrane proteins, even at 60 kHz MAS and a sample temperature of 35 °C. Such couplings are presumably substantial in KcsA owing to the presence of large internal water-filled cavities and buried water.[3c]

Notably, the high spectral quality conferred by our two-step approach even allows measuring the TM part of KcsA directly in a native cell membrane.[10] Cellular membranes are much more complex than reconstituted lipid bilayers in terms of the lipid and protein composition, and this can influence membrane protein function. However, adequate spectral quality is a challenge in cellular ssNMR studies owing to the low concentration of the target protein. Cellular iFD KcsA was expressed in the *E. coli* inner membrane using rifampicin to ensure selective ^{13}C,^{15}N-labeling of KcsA and reduce the endogenous spectral background.[11] The outer membrane was removed to increase the amount of KcsA in the sample, which was then incubated in deuterated solvent for three days prior to the ssNMR experiments. We obtained a surprisingly well-resolved in situ 2D NH spectrum (Figure 2E), which exhibited the clear spectral fingerprint of closed-conductive KcsA[9c] without any discernible background signal (Figure S6). This is remarkable as the KcsA concentration in situ was about seven times lower than in vitro (see Section S10 in the Supporting Information). We could readily annotate the in situ spectrum based on our in vitro assignments (see below). To the best of our knowledge, this is the first time that a few nanomoles of a membrane protein (that is, ca. 3 nanomoles of KcsA, corresponding to ca. 175 μg of protein) could be assigned in situ with ^1H-detected ssNMR spectroscopy. Cellular KcsA showed only small chemical shift perturbations (CSPs) compared to reconstituted KcsA (Figure S11), implying that *E. coli* lipids are good membrane mimics. Yet, we observed a few marked differences in situ, which we discuss below, together with the assignments and relaxation studies performed in vitro. In addition, many signals in the in situ spectrum are strongly broadened by up to 100% (Figure S7), which arises from inhomogeneous line broadening owing to the cellular heterogeneity. This type of broadening is independent of the MAS frequency and likely impacts on sensitivity when using smaller (< 1.3 mm) rotor diameters.

We could assign approximately half of the resonances in the spectrum in Figure 2B based on 3D CαNH, Cα(CO)NH, CONH, and CO(Cα)NH experiments (Figure 2F), supplemented with 3D NCαCX and 2D N(CO)CX spectra to identify residue types, and supported by available ^{13}C and ^{15}N chemical-shift data.[9c,12] These assignments include a number of functionally essential structural elements that we can access here for the first time with ^1H detection.

The selectivity filter, responsible for the stringent selection of K^+ over Na^+ ions, comprises the 75-TVGYG-79 signature sequence, which is common to all K^+ channels.[9a] Whereas only the exchangeable Y78 and G79 residues were detectable in a former study,[2f] here we could also assign residues T74–G77, providing access to the entire filter. Moreover, we assigned the pore helix L66–E71, a critical element for C-type inactivation,[9a] as well as large stretches of the TM1 (transmembrane 1) helix including residues L41–L49, which precede the lipid-sensitive turret.[9c] These signals could be largely retrieved in cellular KcsA. However, we could not unambiguously assign residues of the inner TM2 (transmembrane 2) helix, which was partly due to spectral overlap. Yet, while certain TM2 residues (such as V93–V95) were identified in the spectrum in Figure 2B, our data suggest that the TM2 helix partly exchanges with D_2O, especially C-terminal of the flexible hinge G104.[9a] This hypothesis was corroborated by a 2D N(CO)CX experiment in D_2O with short initial ^1H–^{15}N CP times,[5] in which G104 and G116 could not be observed (Figure S8), and it is in line with studies in micelles.[13] It was also corroborated by the observation of only about 50 signals in the 3D CαNH spectrum although we should observe approximately 65 resonances if all TM H^N were retained in D_2O. H/D exchange within the membrane is hence a curse and a blessing at the same time. Whereas it complicates assignments owing to missing sequential contacts, it can give insight into protein flexibility and membrane topology.

We used our assignments to perform a detailed analysis of the motion in the TM part of KcsA. Understanding this motion is of high relevance for the ion channel function, which depends on dynamic changes of membrane-embedded structural elements.[9a,14] It is also of particular interest to decipher the motion of the filter as its flexibility is assumed to be related to a ubiquitous ion channel regulatory mechanism known as modal gating.[9b] NMR relaxation is a powerful method to study protein dynamics,[15] and many of our assigned H^N signals are well-resolved (Figure 2B), which is a prerequisite for site-resolved analysis. It has previously been shown that ^{15}N transverse rotation frame relaxation ($T_{1\rho}$), which is a sensitive reporter of motion on the nano- to microsecond timescale, can be quantitatively extracted in fully protonated samples at higher (> 50 kHz) MAS frequencies,[16] at which coherent contributions to the magnetization decay are largely suppressed. We first measured the bulk ^{15}N $T_{1\rho}$ as a function of the spinlock amplitude (Figure S9). In agreement with measurements in GB1 and membrane protein ASR,[16–17] we found a relaxation plateau for spinlock fields from about 10 to 25 kHz, yielding a bulk ^{15}N $T_{1\rho}$ of approximately 100 ms for the TM part of KcsA. The site-resolved ^{15}N $T_{1\rho}$ relaxation rates ($R_{1\rho}$) show a rather uniform dynamic regime for the lipid-confined TM part, which is in line with the measurements in micelles[18] (Figures 3A,B).

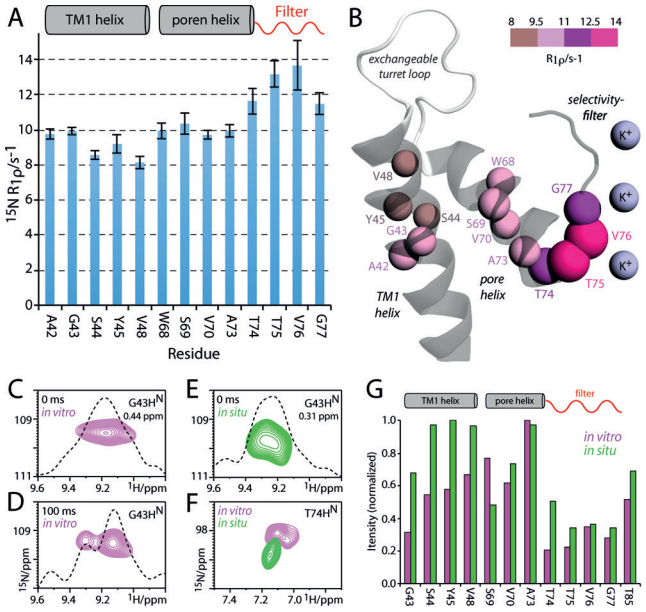

Figure 3. Dynamics recorded for the TM part of D_2O-washed iFD KcsA. All data were acquired at 60 kHz MAS and 800 MHz using a ^{15}N spinlock field of 20 kHz. A) ^{15}N $R_{1\rho}$ relaxation rates. B) Illustration of the ^{15}N $R_{1\rho}$ rates on the KcsA structure (PDB No. 1K4C). Analyzed residues are shown as color-coded spheres whose size is proportional to $R_{1\rho}$. C, D) ^{15}N $T_{1\rho}$ experiments in vitro with a spinlock duration of C) 0 ms or D) 100 ms reveal two signals for $G43H^N$. E) $G43H^N$ exhibits only one conformation in situ. F) T74 showed a ^{15}N chemical shift perturbation of +0.8 ppm in situ. G) Signal-to-noise ratios of resolved residues in in vitro (magenta) and in situ (green) D_2O-washed KcsA.

However, the entire filter stretch T74–G77 remarkably features modestly, but clearly enhanced ^{15}N $R_{1\rho}$, which is indicative of slow and presumably collective molecular motion. This motion very likely corresponds to slow nanosecond to microsecond dynamics as residues T74 and T75 did not show increased fast nanosecond motion in a previous ^{15}N T_1 relaxation study.[19] Such slow motions have not been observed before in membrane-embedded KcsA and can be important for its function as the filter backbone is immediately involved in ion conductance. Interestingly, flicker transitions,[9b] a form of modal gating represented by rapid channel opening and closure, also occur on the microsecond timescale, and flickering is indeed thought to be related to dynamic rearrangements around V76. Increased filter dynamics were also corroborated by reduced signal intensities in dipolar experiments (Figure 3G). The conformational flexibility is also reflected in the H^N linewidth, which is consistently larger for the filter than for the pore helix (Table S5). The TM1 helix residues A42–L49 are least subjected to slow motion and feature slightly smaller $R_{1\rho}$ rates than the pore helix. However, the $G43H^N$ resonance, which is by far the broadest of all H^N (0.44 ppm), is split into two signals with different relaxation decays (Figures 3C,D). As the G43 chemical shift is sensitive to the filter ion-binding mode,[12] this splitting may hence also be related to the conformational flexibility of the filter. Intriguingly, unlike almost all other resonances, the $G43H^N$ resonance is much narrower (0.31 ppm) in situ, most likely because only one conformation is present (Figure 3E). This finding suggests that the KcsA conformational dynamics are, at least locally, altered in native bacterial membranes compared to liposomes.

While the spectral sensitivity inhibits site-resolved relaxation studies in cellular KcsA, an analysis of signal intensities in dipolar experiments showed the lowest intensities for residues T74–G77. This result strongly suggests that the enhanced filter dynamics are maintained in the native membrane (Figure 3G). In fact, the conformational flexibility of the filter seems to be further enhanced in situ as the filter signals are much reduced compared to those of the TM1 helix. Remarkably, also the relative intensities of the filter residues are changed, especially for T74, which displays the lowest intensity of all filter residues in vitro and by far the highest sensitivity in situ. This suggests that the dynamics of the filter are changed in cellular KcsA, which is further corroborated by a relatively strong ^{15}N CSP of +0.8 ppm for T74 in situ (Figures 3F and S11). A potential reason for this apparently different behavior of the filter may be the altered lipid composition in the bacterial membrane, which is known to influence the filter,[9c] or differential clustering of KcsA channels.[20] Against the backdrops presented here, it is of great importance to explore how molecular motion modulates channel function. Whereas our data clearly show enhanced filter dynamics, further extensive measurements will be necessary to fully understand the timescales and amplitudes of these dynamics.

In conclusion, we have introduced an approach that enables the ^1H detection of water-inaccessible proteins with high sensitivity and resolution. We expect our method to be especially powerful for the study of membrane proteins and amyloid fibrils, which both exhibit domains that are highly resistant to hydrogen/deuterium exchange. Moreover, our method allows for the first time the use of ^1H detection for the detailed analysis of a membrane protein in native cell membranes. This constitutes an important advance in ssNMR spectroscopy as membrane protein function often critically depends on the native environment.

Acknowledgements

We acknowledge support by the NWO (projects 723.014.003, 700.10.443, 184.032.207). Experiments at the 950 MHz instrument were supported by uNMR-NL, an NWO-funded National Roadmap Large-Scale Facility of the Netherlands.

Keywords: in-cell NMR spectroscopy · membrane proteins · protein dynamics · proton detection · solid-state NMR spectroscopy

How to cite: *Angew. Chem. Int. Ed.* **2016**, *55*, 13606–13610
Angew. Chem. **2016**, *128*, 13804–13808

[1] Y. Ishii, R. Tycko, *J. Magn. Reson.* **2000**, *142*, 199–204.
[2] a) V. Chevelkov, K. Rehbein, A. Diehl, B. Reif, *Angew. Chem. Int. Ed.* **2006**, *45*, 3878–3881; *Angew. Chem.* **2006**, *118*, 3963–3966; b) P. Schanda, B. H. Meier, M. Ernst, *J. Am. Chem. Soc.* **2010**, *132*, 15957–15967; c) R. Linser, M. Dasari, M. Hiller, V. Higman, U. Fink, J. M. Lopez del Amo, S. Markovic, L. Handel,

B. Kessler, P. Schmieder, D. Oesterhelt, H. Oschkinat, B. Reif, *Angew. Chem. Int. Ed.* **2011**, *50*, 4508 – 4512; *Angew. Chem.* **2011**, *123*, 4601 – 4605; d) M. E. Ward, L. Shi, E. Lake, S. Krishnamurthy, H. Hutchins, L. S. Brown, V. Ladizhansky, *J. Am. Chem. Soc.* **2011**, *133*, 17434 – 17443; e) V. Chevelkov, B. Habenstein, A. Loquet, K. Giller, S. Becker, A. Lange, *J. Magn. Reson.* **2014**, *242*, 180 – 188; f) D. Mance, T. Sinnige, M. Kaplan, S. Narasimhan, M. Daniels, K. Houben, M. Baldus, M. Weingarth, *Angew. Chem. Int. Ed.* **2015**, *54*, 15799 – 15803; *Angew. Chem.* **2015**, *127*, 16025 – 16029; g) H. R. Dannatt, M. Felletti, S. Jehle, Y. Wang, L. Emsley, N. E. Dixon, A. Lesage, G. Pintacuda, *Angew. Chem. Int. Ed.* **2016**, *55*, 6638 – 6641; *Angew. Chem.* **2016**, *128*, 6750 – 6753; h) T. Sinnige, M. Daniels, M. Baldus, M. Weingarth, *J. Am. Chem. Soc.* **2014**, *136*, 4452 – 4455.

[3] a) D. H. Zhou, G. Shah, M. Cormos, C. Mullen, D. Sandoz, C. M. Rienstra, *J. Am. Chem. Soc.* **2007**, *129*, 11791 – 11801; b) A. Marchetti, S. Jehle, M. Felletti, M. J. Knight, Y. Wang, Z. Q. Xu, A. Y. Park, G. Otting, A. Lesage, L. Emsley, N. E. Dixon, G. Pintacuda, *Angew. Chem. Int. Ed.* **2012**, *51*, 10756 – 10759; *Angew. Chem.* **2012**, *124*, 10914 – 10917; c) M. Weingarth, E. A. van der Cruijsen, J. Ostmeyer, S. Lievestro, B. Roux, M. Baldus, *J. Am. Chem. Soc.* **2014**, *136*, 2000 – 2007; d) S. Wang, S. Parthasarathy, Y. Xiao, Y. Nishiyama, F. Long, I. Matsuda, Y. Endo, T. Nemoto, K. Yamauchi, T. Asakura, M. Takeda, T. Terauchi, M. Kainosho, Y. Ishii, *Chem. Commun.* **2015**, *51*, 15055 – 15058; e) S. Xiang, J. Biernat, E. Mandelkow, S. Becker, R. Linser, *Chem. Commun.* **2016**, *52*, 4002 – 4005.

[4] a) V. Agarwal, S. Penzel, K. Szekely, R. Cadalbert, E. Testori, A. Oss, J. Past, A. Samoson, M. Ernst, A. Bockmann, B. H. Meier, *Angew. Chem. Int. Ed.* **2014**, *53*, 12253 – 12256; *Angew. Chem.* **2014**, *126*, 12450 – 12453; b) K. H. Mroue, Y. Nishiyama, M. Kumar Pandey, B. Gong, E. McNerny, D. H. Kohn, M. D. Morris, A. Ramamoorthy, *Sci. Rep.* **2015**, *5*, 11991.

[5] L. C. Shi, I. Kawamura, K. H. Jung, L. S. Brown, V. Ladizhansky, *Angew. Chem. Int. Ed.* **2011**, *50*, 1302 – 1305; *Angew. Chem.* **2011**, *123*, 1338 – 1341.

[6] R. Verel, M. Baldus, M. Ernst, B. H. Meier, *Chem. Phys. Lett.* **1998**, *287*, 421 – 428.

[7] D. H. Zhou, C. M. Rienstra, *J. Magn. Reson.* **2008**, *192*, 167 – 172.

[8] M. Weingarth, G. Bodenhausen, P. Tekely, *J. Magn. Reson.* **2009**, *199*, 238 – 241.

[9] a) L. G. Cuello, V. Jogini, D. M. Cortes, E. Perozo, *Nature* **2010**, *466*, 203 – 208; b) S. Chakrapani, J. F. Cordero-Morales, V. Jogini, A. C. Pan, D. M. Cortes, B. Roux, E. Perozo, *Nat. Struct. Mol. Biol.* **2011**, *18*, 67 – 74; c) E. A. van der Cruijsen, D. Nand, M. Weingarth, A. Prokofyev, S. Hornig, A. A. Cukkemane, A. M. Bonvin, S. Becker, R. E. Hulse, E. Perozo, O. Pongs, M. Baldus, *Proc. Natl. Acad. Sci. USA* **2013**, *110*, 13008 – 13013.

[10] a) M. Renault, R. Tommassen-van Boxtel, M. P. Bos, J. A. Post, J. Tommassen, M. Baldus, *Proc. Natl. Acad. Sci. USA* **2012**, *109*, 4863 – 4868; b) P. Schanda, S. Triboulet, C. Laguri, C. M. Bougault, I. Ayala, M. Callon, M. Arthur, J. P. Simorre, *J. Am. Chem. Soc.* **2014**, *136*, 17852 – 17860; c) S. A. Shahid, M. Nagaraj, N. Chauhan, T. W. Franks, B. Bardiaux, M. Habeck, M. Orwick-Rydmark, D. Linke, B. J. van Rossum, *Angew. Chem. Int. Ed.* **2015**, *54*, 12602 – 12606; *Angew. Chem.* **2015**, *127*, 12792 – 12797.

[11] L. A. Baker, M. Daniels, E. A. W. van der Cruijsen, G. E. Folkers, M. Baldus, *J. Biomol. NMR* **2015**, *62*, 199 – 208.

[12] B. J. Wylie, M. P. Bhate, A. E. McDermott, *Proc. Natl. Acad. Sci. USA* **2014**, *111*, 185 – 190.

[13] J. H. Chill, J. M. Louis, C. Miller, A. Bax, *Protein Sci.* **2006**, *15*, 684 – 698.

[14] K. Takeuchi, H. Takahashi, S. Kawano, I. Shimada, *J. Biol. Chem.* **2007**, *282*, 15179 – 15186.

[15] a) J. M. Lamley, C. Oster, R. A. Stevens, J. R. Lewandowski, *Angew. Chem. Int. Ed.* **2015**, *54*, 15374 – 15378; *Angew. Chem.* **2015**, *127*, 15594 – 15598; b) P. Ma, Y. Xue, N. Coquelle, J. D. Haller, T. Yuwen, I. Ayala, O. Mikhailovskii, D. Willbold, J. P. Colletier, N. R. Skrynnikov, P. Schanda, *Nat. Commun.* **2015**, *6*, 8361.

[16] J. R. Lewandowski, H. J. Sass, S. Grzesiek, M. Blackledge, L. Emsley, *J. Am. Chem. Soc.* **2011**, *133*, 16762 – 16765.

[17] D. B. Good, S. L. Wang, M. E. Ward, J. Struppe, L. S. Brown, J. R. Lewandowski, V. Ladizhansky, *J. Am. Chem. Soc.* **2014**, *136*, 2833 – 2842.

[18] J. H. Chill, J. M. Louis, J. L. Baber, A. Bax, *J. Biomol. NMR* **2006**, *36*, 123 – 136.

[19] C. Ader, O. Pongs, S. Becker, M. Baldus, *Biochim. Biophys. Acta Biomembr.* **2010**, *1798*, 286 – 290.

[20] A. Sumino, D. Yamamoto, M. Iwamoto, T. Dewa, S. Oiki, *J. Phys. Chem. Lett.* **2014**, *5*, 578 – 584.

Received: July 11, 2016
Revised: September 4, 2016
Published online: September 27, 2016

